PHYSICAL REVIEW C VOLUME 34, NUMBER 4 OCTOBER 1986

Analyzing powers for ($\vec{p}$,2p) reactions with effective N-N interactions

Yoshiteru Kudo and Kiro Miyazaki
Department of Physics, Osaka City University, Sumiyoshi-ku, Osaka 558, Japan
(Received 21 April 1986)

Analyzing powers and cross sections are calculated for the $^{16}O(\vec{p},2p)$ and $^{40}Ca(\vec{p},2p)$ reactions at an incident energy of $E_p=200$ MeV within the framework of the distorted wave impulse approximation, including both the effect of the spin-orbit interaction for the distorted waves and the off-shell effect in the proton-proton scattering. The antisymmetrized t-matrix elements are calculated with the effective nucleon-nucleon interactions by Love and Franey. Our calculations agree well with the experimental data. Although there are substantial contributions from the spin-orbit and the tensor parts in the effective nucleon-nucleon interaction to the cross section, the contribution from the central part is quite weak. Furthermore, we study the medium effects using the density-dependent t-matrix interactions by von Geramb and Nakano. It is found that the medium effects increase the cross sections somewhat, but scarcely change the analyzing powers.

I. INTRODUCTION

For many years the study[1-6] of the (p,2p) reactions has given information about the separation energies and the angular momenta of the proton-hole states in nuclei. Experimentally, the summed energy spectra, the angular correlation cross section, and the energy sharing correlation cross section have been measured corresponding to various combinations of kinematic variables associated with two outgoing protons detected in coincidence. Theoretical analyses of the (p,2p) reactions at bombarding energies greater than 100 MeV have commonly been made by using the distorted wave impulse approximation (DWIA). In the impulse approximation, the effective nucleon-nucleon (N-N) interaction for the (p,2p) reactions is described by the t matrix for free N-N scattering at an energy near that of the reaction. Furthermore, it is assumed that multiple-scattering effects are well reproduced by the distorted waves and that the reaction process may then be described by a single-step mechanism. To the extent that the reaction dynamics are well understood, attention may then be focused on extracting nuclear structure information. We can determine the separation energies of the proton-hole states from the positions of the peaks in the summed energy spectrum of the two outgoing protons. The shapes of the distributions of the correlation cross section which are very sensitive to the shell model configurations give information about the angular momenta of these proton-hole states.

Recently, interest has been renewed in this field[6-13] by the start of experimental studies using a polarized proton beam. Polarization data are expected to be particularly sensitive to the spin-dependent portions of the effective interaction. They will also depend on the optical potentials used in the calculation of reaction processes. Experimental measurements of analyzing powers and cross sections for the $^{16}O(\vec{p},2p)$ reaction by Kitching *et al.*[14] and for the $^{40}Ca(\vec{p},2p)$ reaction by Antonuk *et al.*[15] at TRIUMF have shown the strong dependence of the analyzing power on the J value of the proton-hole state. The experimental data have been compared with DWIA calculations[14,15] by the TRIUMF group with a half-off-shell prescription for the free p-p scattering matrix element, in which the free t matrix is factorized into two parts: the on-shell t matrix and a real off-shell extension function. However, in some cases of the analyzing powers and cross sections, significant discrepancies between the experimental results and the calculated ones have been shown. The discrepancies seem to be attributable to possible problems with the effective N-N interaction and the factorization assumption.

Recently, great progress[16] has been made in the construction of two types of the effective N-N interactions: one type involves t-matrix interactions based directly on phenomenological N-N scattering amplitudes, and the other involves G-matrix (density dependent t matrix) interactions derived from N-N potentials which describe N-N scattering observables or phase shifts. The effective N-N interactions have been applied to the descriptions of N-nucleus elastic and inelastic scatterings and they have provided useful information about reaction processes and nuclear structures. The applications of such N-N effective interactions may also be useful for studying the (p,2p) reactions and may be expected to provide complementary information to N-nucleus scattering.

In the present paper the cross section and the analyzing power are calculated in the DWIA using the t-matrix interaction of Love and Franey (LF interaction).[17,18] We take into account both the effect of the spin-orbit interaction for the distorted waves and the off-shell effect in the proton-proton scattering. Furthermore, in order to study the medium effects, we calculated the cross section and the analyzing power using the effective G-matrix interaction of von Geramb and Nakano (GN interaction).[19]

Numerical calculations are carried out for the analyzing powers and the cross sections for the $1p_{3/2}$ and $1p_{1/2}$ states for the $^{16}O(\vec{p},2p)$ reaction[14] and for the $1d_{5/2}$ and $1d_{3/2}$ states for the $^{40}Ca(\vec{p},2p)$ reaction[15] at $E=200$ MeV by the TRIUMF group.

In Sec. II the expressions for the cross section and the analyzing power used in the analyses are derived. The numerical results and some discussions are given in Sec. III. The last section is devoted to a summary and conclusion of this paper. In the Appendix the expression of the off-shell N-N t matrix is presented. Preliminary results of this work have been reported in Ref. 20.

II. CROSS SECTION AND ANALYZING POWER

In the coplanar geometry of the $A(a,ab)C$ reaction, the outgoing particles a and b are detected in coincidence at angles θ_a and θ_b, respectively, on opposite sides of the incident particle and with the incident and outgoing particles in the same plane. In this paper, the particles a and b mean protons. The momenta (kinetic energies) of the incident particle a and outgoing particles a and b are $\hbar\mathbf{k}_0(E_0)$, $\hbar\mathbf{k}_a(E_a)$, and $\hbar\mathbf{k}_b(E_b)$, respectively, in the lab system. The cross section[21] is then given by

$$\frac{d^3\sigma}{d\Omega_a d\Omega_b dE_a}=\frac{F_{\rm kin}}{(2s_a+1)(2J_A+1)}\sum_{(\gamma_1)}|T_{fi}|^2 , \tag{2.1}$$

where the kinematical factor $F_{\rm kin}$ is

$$F_{\rm kin}=\frac{m_a^2 m_b c^6}{(\hbar c)^6(2\pi)^5}\frac{k_a k_b}{k_0}\times\left|1+\frac{m_b}{m_C}\left[1-\frac{k_0}{k_b}\cos\theta_b+\frac{k_a}{k_b}\cos(\theta_a+\theta_b)\right]\right|^{-1} . \tag{2.2}$$

The spin (projection) quantum numbers of the particle a and the target nucleus A in the initial state are s_a (μ_a) and J_A (M_A), respectively. Also, in the final state, the quantum numbers of the particles a and b and the residual nucleus C are s_a (μ_a'), s_b (μ_b'), and J_C (M_C), respectively. The mass of the particle i is m_i. The summation (γ_1) of the transition matrix T_{fi} in Eq. (2.1) is taken over the spin components μ_a, μ_a', μ_b', M_A, and M_C in the initial and final states.

We can express the transition matrix element[2] in Eq. (2.1) by

$$T_{fi}=\langle\Psi_f^{(-)}|V_{ab}+V_{aC}|\Phi_i\rangle . \tag{2.3}$$

The wave function Φ_i and $\Psi_f^{(-)}$ show the scattering eigenstates of the free Hamiltonian in the initial state and the total Hamiltonian, respectively. The interaction between the particles α and β is $V_{\alpha\beta}$. In the distorted wave formalism, the transition amplitude is given by

$$T_{fi}=\langle\chi_f^{(-)}\Psi_C|\tau_{ab}|\chi_i^{(+)}\Psi_A\rangle . \tag{2.4}$$

In the derivation of this expression, the transition amplitude corresponding to the indirect knock-out processes[22,23] was neglected. Here, Ψ_A and Ψ_C are the wave functions of the target nucleus A and the residual nucleus C, respectively. The distorted wave functions $\chi_i^{(+)}$ and $\chi_f^{(-)}$ are generated by making use of the optical potentials V_{aC} and $V_{aC}+V_{bC}$, including the spin-orbit distortion, respectively. We denote the a-b transition operator by τ_{ab}. It is not the free transition operator but the true transition operator containing the medium effects and describing how the incident particle a is scattered by the bound particle b while both particles a and b interact with the core nucleus C through the potentials V_{aC} and V_{bC} in the total Hamiltonian. If we neglect the medium effects, we can obtain the free transition operator. It differs only kinematically from the operator which describes the scattering of the particle a by the free particle b.

The τ_{ab} operator[17–19] is expressed in the form of a two-nucleon potential which consists of the central, spin-orbit, and tensor parts,

$$\tau_{ab}=\sum_{S,T}(\tau_0^{ST}+\tau_1^{ST}\mathbf{L}\cdot\mathbf{S}+\tau_2^{ST}S_{ab})P^S P^T , \tag{2.5}$$

where the relative orbital angular momentum and the total spin operators in two-nucleon system are denoted $\mathbf{L}$ and $\mathbf{S}$, respectively. Here, S_{ab} and P^S (P^T) are the usual tensor operator and the projection operator of the spin S (isospin T) state, respectively. The radial parts of τ_{ab} are taken to be sums of Yukawa forms $t_{k,i}(r_{ab})$ ($k=0$, 1, or 2) with different ranges R_i,

$$\tau_k^{ST}=\sum_i V_{k,i}^{ST}(E,\rho(R))t_{k,i}(r_{ab}) , \tag{2.6}$$

where the interaction strengths $V_{ki}^{ST}(E,\rho(R))$ are complex and depend on the nucleon incident energy E and the target density $\rho(R)$ at $\mathbf{R}=(\mathbf{r}_{aC}+\mathbf{r}_{bC})/2$. The τ_{ab} operator, in general, depends on the nuclear density $\rho(R)$ as in the GN interaction, but in the special case of a free interaction, such as the LF interaction, it is independent of the density.

By choosing the two variables $\mathbf{r}_{aC}$ and $\mathbf{r}_{bC}$, the transition matrix element in Eq. (2.4) can be written, after integration on the internal coordinates, as

$$T_{fi}=n_A^{-1/2}C\sum_{LJ\Lambda}\Theta_{LJ}(C,b\,|\,A)(Ls_b\Lambda\mu_b\,|\,JM)(JJ_CMM_C\,|\,J_AM_A)T_{JL\Lambda}(\mu_a'\mu_b':\mu_a\mu_b) , \tag{2.7}$$

where

$$T_{JL\Lambda}(\mu_a'\mu_b':\mu_a\mu_b)=\sum_{\sigma_a\sigma_a'\sigma_b'}\int d\mathbf{r}_{aC}d\mathbf{r}_{bC}\chi_{\sigma_a'\mu_a'}^{(-)*}(\mathbf{k}_{aC},\mathbf{r}_{aC})\chi_{\sigma_b'\mu_b'}^{(-)*}(\mathbf{k}_{bC},\mathbf{r}_{bC})\times\langle\sigma_a'\sigma_b'\,|\,\tau_{ab}\,|\,\sigma_a\mu_b\rangle\chi_{\sigma_a\mu_a}^{(+)}(\mathbf{k}_{aA},\mathbf{r}_{aA})\Phi_{JL\Lambda}(\mathbf{r}_{bC}) , \tag{2.8}$$

with $C=(t_bT_C\nu_bN_C\,|\,T_AN_A)$, $\mathbf{k}_{aA}=m_A\mathbf{k}_0/m$, $\mathbf{k}_{aC}=\mathbf{k}_a-m_a\mathbf{k}_0/m$, $\mathbf{k}_{bC}=\mathbf{k}_b-m_b\mathbf{k}_0/m$, and $m=m_a+m_b+m_C$.

The distorted wave function $\chi^{(\pm)}_{\sigma_i\mu_i}(\mathbf{k}_{\alpha\beta},\mathbf{r}_{\alpha\beta})$ of the particle i is generated by making use of the optical potential $V_{\alpha\beta}$. The relative coordinate vector between particles α and β is $\mathbf{r}_{\alpha\beta}$ and the required conjugate momentum in the total c.m. system[24] is $\hbar\mathbf{k}_{\alpha\beta}$. The fractional parentage coefficient for the decomposition for $A\to b+C$ is $\Theta_{LJ}(C,b\,|\,A)$ and n_A denotes the number of nucleons in the nucleus A. The relative wave function for $b+C$ is $\Phi_{JL\Lambda}(\mathbf{r}_{bC})$ with the quantum number $JL\Lambda$. The isospin (projection) quantum numbers of the particle b, the core nucleus C, and the target nucleus A are t_b (ν_b), T_C (N_C), and T_A (N_A), respectively. For the sake of simplicity, we omit the isospin quantum numbers in $\langle\,|\tau_{ab}|\,\rangle$ in Eq. (2.8).

In order to reduce the six-dimensional integration of Eq. (2.8) to the three-dimensional one, we introduce Fourier transforms of the various wave functions, as does the usual DWIA,[25] and rewrite Eq. (2.8) as follows,

$$T_{JL\Lambda}(\mu_a'\mu_b';\mu_a\mu_b)=\sum_{\sigma_a\sigma_a'\sigma_b'}(2\pi)^{-3}\int d\mathbf{q}_{aA}d\mathbf{q}_{aC}d\mathbf{q}_{bC}d\mathbf{Q}_{bC}\delta(\alpha\mathbf{q}_{aA}-\mathbf{q}_{aC}-\mathbf{q}_{bC}+\mathbf{Q}_{bC})$$
$$\times\widetilde{\chi}^{(-)*}_{\sigma_a'\mu_a'}(\mathbf{k}_{aC},\mathbf{q}_{aC})\widetilde{\chi}^{(-)*}_{\sigma_b'\mu_b'}(\mathbf{k}_{bC},\mathbf{q}_{bC})\widetilde{\chi}^{(+)}_{\sigma_a\mu_a}(\mathbf{k}_{aA},\mathbf{q}_{aA})\widetilde{\Phi}_{JL\Lambda}(\mathbf{Q}_{bC})$$
$$\times\langle\mathbf{q}^{(f)}_{ab};\sigma_a'\sigma_b'\,|\,\tau_{ab}\,|\,\mathbf{q}^{(i)}_{ab};\sigma_a\mu_b\rangle\,, \tag{2.9}$$

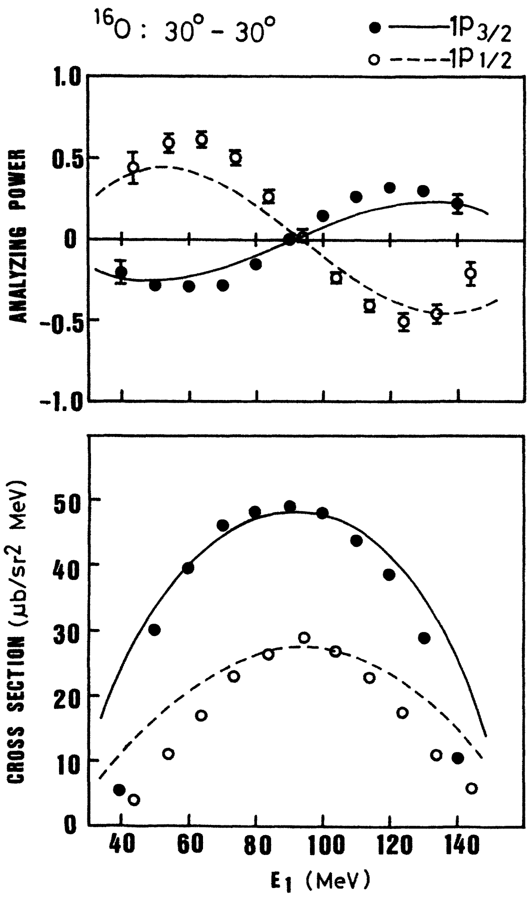

FIG. 1. The calculated results and the experimental data of the cross section and the analyzing power at angle pair ($\theta_a=\theta_b=30°$) for the $1p_{3/2}$ and $1p_{1/2}$ states for the ^{16}O($\vec{p}$,2p) reaction at $E_p=200$ MeV. The experimental data (Ref. 14) for the $1p_{3/2}$ (●) and $1p_{1/2}$ (○) states are presented as a function of the kinetic energy (E_1) of one of the final state protons. The calculated results with the LF interaction for the $1p_{3/2}$ and $1p_{1/2}$ states are given as solid and dashed lines, respectively.

where $\widetilde{\chi}^{(\pm)}_{\mu_i\mu_i'}$ and $\widetilde{\Phi}_{JL\Lambda}$ correspond to Fourier transforms of the wave functions $\chi^{(\pm)}_{\mu_i\mu_i'}$ and $\Phi_{JL\Lambda}$, respectively, and $\alpha=m_C/(m_b+m_C)$. The factor

$$\langle\mathbf{q}^{(f)}_{ab};\sigma_a'\sigma_b'\,|\,\tau_{ab}\,|\,\mathbf{q}^{(i)}_{ab};\sigma_a\mu_b\rangle$$

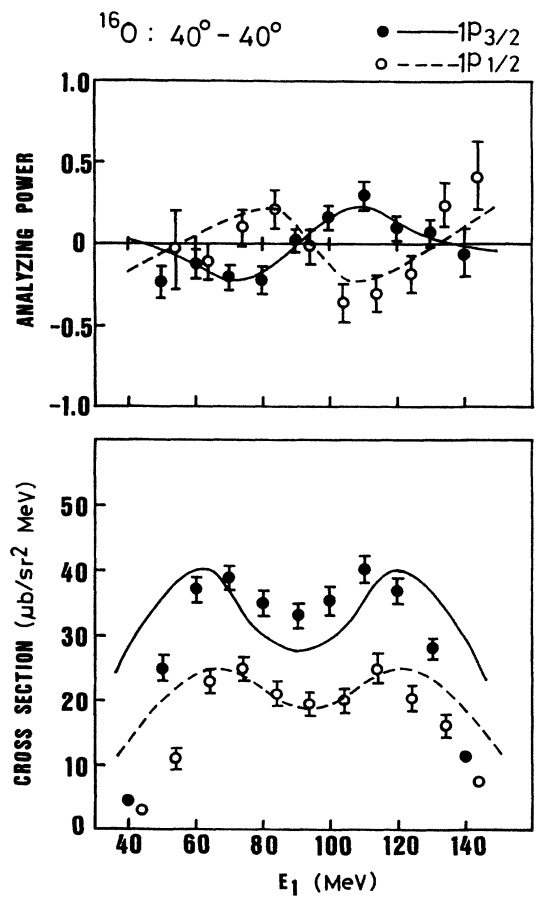

FIG. 2. Same as Fig. 1, except ($\theta_a=\theta_b=40°$).

is the off-shell a-b t-matrix element with the initial and final momenta $\mathbf{q}_{ab}^{(i)}$ and $\mathbf{q}_{ab}^{(f)}$, respectively,

$$\mathbf{q}_{ab}^{(i)}=\mathbf{q}_{aA}-m_a(\mathbf{q}_{aC}+\mathbf{q}_{bC})/(m_a+m_b) \tag{2.10}$$

and

$$\mathbf{q}_{ab}^{(f)}=(m_b\mathbf{q}_{aC}-m_a\mathbf{q}_{bC})/(m_a+m_b)\ . \tag{2.11}$$

If we approximate this t-matrix element by the one with the asymptotic initial and final momenta $\mathbf{k}_{ab}^{(i)}$ and $\mathbf{k}_{ab}^{(f)}$, respectively (hereafter, we call this approximation the asymptotic momentum approximation),

$$\langle \mathbf{q}_{ab}^{(f)};\sigma_a'\sigma_b' \mid \tau_{ab} \mid \mathbf{q}_{ab}^{(i)};\sigma_a\mu_b \rangle \sim \langle \mathbf{k}_{ab}^{(f)};\sigma_a'\sigma_b' \mid \tau_{ab} \mid \mathbf{k}_{ab}^{(i)};\sigma_a\mu_b \rangle \tag{2.12}$$

where

$$\mathbf{k}_{ab}^{(i)}=\mathbf{k}_0-m_a(\mathbf{k}_a+\mathbf{k}_b)/(m_a+m_b) \tag{2.13}$$

and

$$\mathbf{k}_{ab}^{(f)}=(m_b\mathbf{k}_a-m_a\mathbf{k}_b)/(m_a+m_b)\ , \tag{2.14}$$

then we can easily obtain the transition matrix element with three-dimensional integration,

$$T_{JL\Lambda}(\mu_a'\mu_b';\mu_a\mu_b)=\sum_{\sigma_a\sigma_a'\sigma_b'}\int d\mathbf{r}\,\chi^{(-)*}_{\sigma_a'\mu_a'}(\mathbf{k}_{aC},\mathbf{r})\chi^{(-)*}_{\sigma_b'\mu_b'}(\mathbf{k}_{bC},\mathbf{r}) \times\langle \mathbf{k}_{ab}^{(f)};\sigma_a'\sigma_b' \mid \tau_{ab} \mid \mathbf{k}_{ab}^{(i)};\sigma_a\mu_b \rangle_a \chi^{(+)}_{\sigma_a\mu_a}(\mathbf{k}_{aA},\alpha\mathbf{r})\Phi_{JL\Lambda}(\mathbf{r})\ . \tag{2.15}$$

Thus, we can modify the ordinary DWIA expression[12,21] so as to take into account the medium effects. Our result differs from those[12,21] obtained earlier in that the τ_{ab} transition matrix elements depend not only on the

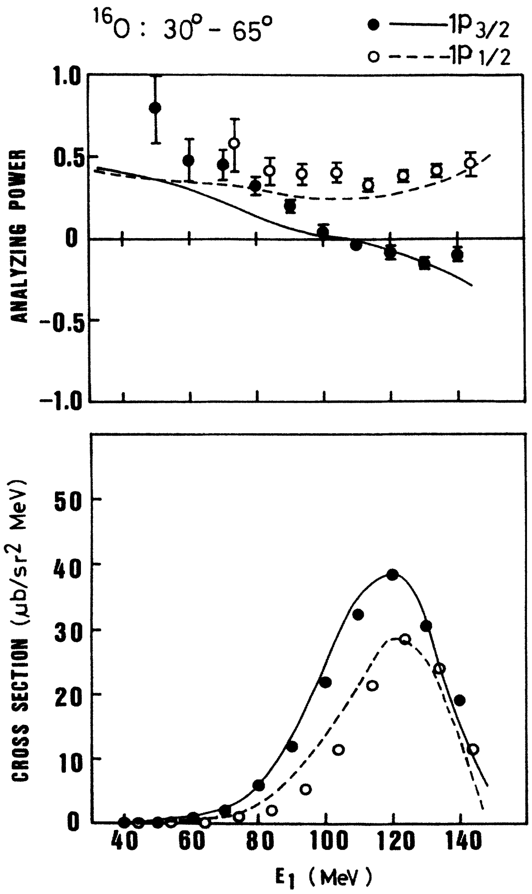

FIG. 3. Same as Fig. 1, except ($\theta_a=30°$, $\theta_b=65°$).

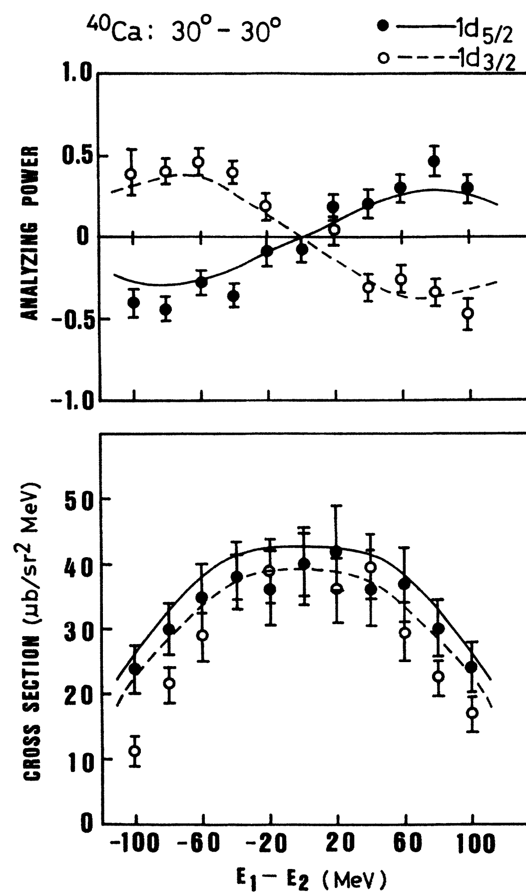

FIG. 4. The calculated results and the experimental data of the cross section and the analyzing power at angle pair ($\theta_a=\theta_b=30°$) for the $1d_{5/2}$ and $1d_{3/2}$ states for the ^{40}Ca($\vec{p}$,2p) reaction at $E_p=200$ MeV. The experimental data (Ref. 15) for the $1d_{5/2}$ (●) and $1d_{3/2}$ (○) states are presented as a function of the difference (E_1-E_2) between the kinetic energies of the two outgoing protons. The calculated results with the LF interaction for the $1d_{5/2}$ and $1d_{3/2}$ states are given as solid and dashed lines, respectively.

momenta $\mathbf{k}_{ab}^{(i)}$ and $\mathbf{k}_{ab}^{(f)}$ but also on the coordinate $\mathbf{r}$. When the τ_{ab} matrix elements do not depend on the coordinate, Eq. (2.15) coincides with the expression of the ordinary DWIA. The $\langle \mid \tau_{ab} \mid \rangle_a$ in Eq. (2.15) are the antisymmetrized off-shell a-b t-matrix elements, which are given explicitly in the Appendix.

We obtain the expression for the cross section of Eq. (2.1) for specific values of L and J,

$$\frac{d^3\sigma}{d\Omega_a d\Omega_b dE_a} = F_{\text{kin}} \frac{S_{LJ}}{(2s_a+1)(2J+1)} \sum_{(\gamma_2)} \left| \sum_{\mu_b} (Ls_b\Lambda\mu_b \mid JM) T_{JL\Lambda}(\mu_a'\mu_b' ; \mu_a\mu_b) \right|^2 , \tag{2.16}$$

with $(\gamma_2)=(\mu_a,\mu_a',\mu_b',M)$, and the expression for the analyzing power is given by

$$A_y = \sum_{(\gamma_3)} (Ls_b\Lambda\mu_b \mid JM)(Ls_b\Lambda'\sigma_b \mid JM) T_{JL\Lambda}(\mu_a'\mu_b' ; \mu_a\mu_b)(\sigma_{ay})_{\mu_a\sigma_a} T^*_{JL\Lambda'}(\mu_a'\mu_b' ; \sigma_a\sigma_b) \Big/ \sum_{(\gamma_1)} \mid T_{fi} \mid^2 , \tag{2.17}$$

with $(\gamma_3)=(\mu_a,\mu_a',\sigma_a,\mu_b,\mu_b',\sigma_b,M)$.

The y component of the Pauli spin operator of the incident particle a is σ_{ay}. Here, the direction of propagation of the incident particle a is parallel to the z axis, and the polarization axis is taken to be the y axis. The spectroscopic factor S_{LJ} is defined by $\mid C\Theta_{LJ}(C,b \mid A) \mid^2$.

In the numerical calculation of Eq. (2.15), we employ a direct three-dimensional numerical integration proposed by Chant and Roos[26] in order to avoid the use of complex angular momentum coupling coefficients and to save a lot of computing time.

III. RESULTS AND DISCUSSIONS

In this section the calculated results are compared with the cross section and the analyzing power data[14,15] at angle pairs ($\theta_a=\theta_b=30°$), ($\theta_a=\theta_b=40°$), and ($\theta_a=30°$, $\theta_b=65°$) for the $1p_{3/2}$ and $1p_{1/2}$ states for the ^{16}O(p,2p) reaction, and at angle pairs ($\theta_a=\theta_b=30°$), ($\theta_a=\theta_b=47°$), and ($\theta_a=29°$, $\theta_b=47°$) for the $1d_{5/2}$ and $1d_{3/2}$ states for the ^{40}Ca(p,2p) reaction, at $E_p=200$ MeV in the coplanar geometry.

We calculate the antisymmetrized off-shell t-matrix ele-

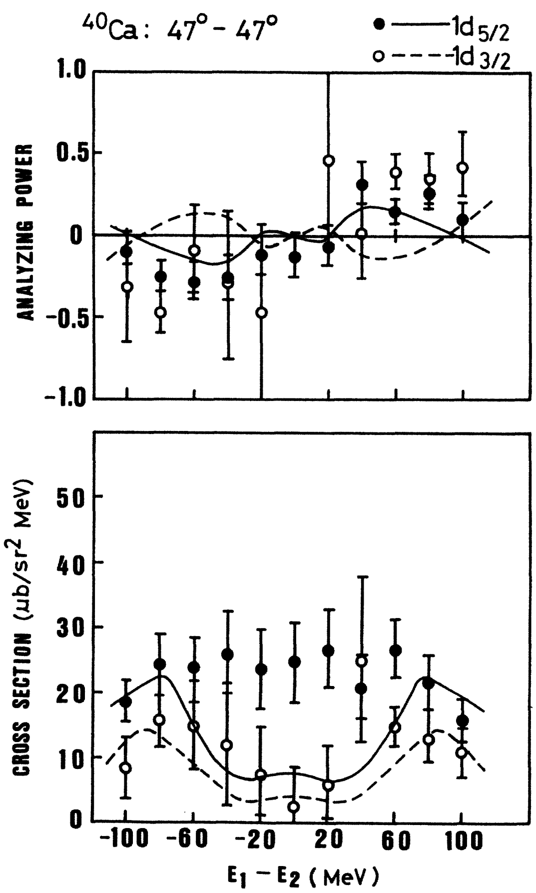

FIG. 5. Same as Fig. 4, except ($\theta_a=\theta_b=47°$).

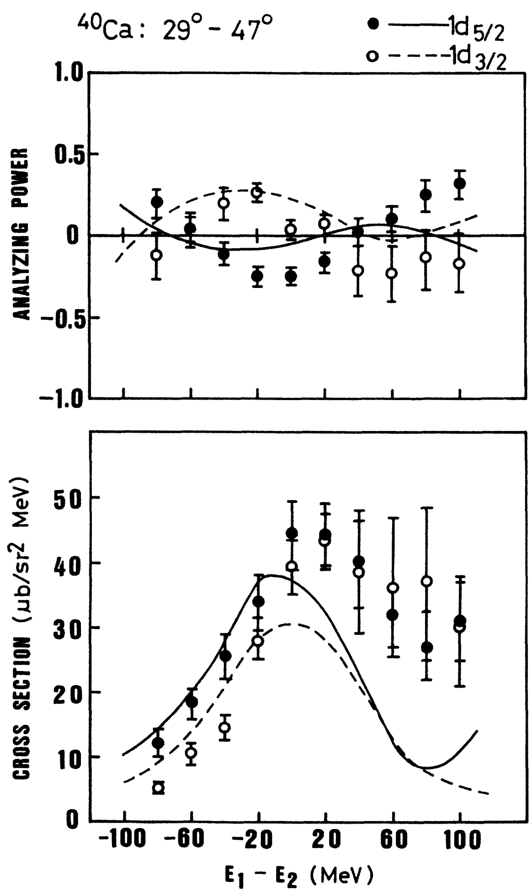

FIG. 6. Same as Fig. 4, except ($\theta_a=29°$, $\theta_b=47°$).

ments in Eq. (2.15) by making use of two types of effective N-N interactions: one is the LF interaction,[17,18] whose parameters are tabulated in Ref. 18, and the other is the GN interaction.[19] The calculation with the former interaction corresponds to the ordinary DWIA treatment.

The *G*-matrix interactions were generated by von Geramb and Nakano from the free N-N Paris potential and parametrized into a complex energy and density dependent interaction with convenient Yukawa form factors. The Fermi motion was taken into account in version 2 of the interaction (GN-2 interaction). In addition to this effect, the Pauli-blocking effect was taken into account in version 3 of the interaction (GN-3 interaction). The parameters for these interactions are tabulated in Ref. 19. We can modify the ordinary DWIA calculation by adopting the GN interaction so as to include nuclear medium effects. In calculations of the (p,p′) scattering, the effective interaction corresponding to the proton bombarding energy is usually used. Therefore, we also used the interaction parameters for proton bombarding energies of 210, 200, and 200 MeV for the LF, GN-2, and GN-3 interactions, respectively.

The radial wave functions of the bound states for a proton in the target nucleus are solved by making use of a real Woods-Saxon potential with a spin-orbit term. The potential parameters are taken from values of Elton and Swift[27] which have been derived from fits to elastic electron scattering data and the binding energy of the particular single particle state.

The parameters of the target densities for ^{16}O and ^{40}Ca in Eq. (2.6) that are necessary for interactions GN-2 and GN-3 are taken from the data[28,29] on charge distributions found from elastic electron scattering. On the other hand, the LF interaction does not depend on the target density.

In order to analyze the experimental data for the (p,2p) reaction, we need the optical potential parameters over a wide range of proton bombarding energies because of the variation of the outgoing proton energies in the final state. The parameters of the proton optical potentials for ^{16}O and ^{40}Ca are constructed by the interpolation method from the parameters of Ref. 30 and Refs. 31—33, respectively.

The experimental cross sections and analyzing powers are represented as a function of the kinetic energy (E_1) of one of the final state protons at each angle pair (θ_a,θ_b) for the ^{16}O($\vec{p}$,2p) reaction and as a function of the difference (E_1-E_2) between the kinetic energies of two outgoing protons at each angle pair (θ_a,θ_b) for the ^{40}Ca($\vec{p}$,2p) reaction, respectively. In the present paper, the cross section values are

$$\frac{d^3\sigma}{d\Omega_a d\Omega_b d(E_a-E_b)}=\frac{1}{2}\frac{d^3\sigma}{d\Omega_a d\Omega_b dE_a}\ , \tag{3.1}$$

where the expression of $d^3\sigma/d\Omega_a d\Omega_b dE_a$ is given by Eq. (2.16). In Figs. 1—8 we show the calculated results only with the LF interaction for the cross sections and the analyzing powers, because the LF, GN-2, and GN-3 interactions give almost the same results, except for the magnitude of the cross section, as will be shown in Fig. 11.

In Figs. 1, 2, and 3 the calculated results with the LF interaction are compared with the data[14] of the cross sections and the analyzing powers at angle pairs ($\theta_a=\theta_b=30°$), ($\theta_a=\theta_b=40°$), and ($\theta_a=30°,\theta_b=65°$), respectively, for the $1p_{3/2}$ and $1p_{1/2}$ states for the ^{16}O($\vec{p}$,2p) reaction. The calculated cross sections and analyzing powers in Figs. 1—3 are in reasonably good agreement with the data. When compared with calculations by Kitching *et al.*,[14] the great improvements for the analyzing powers are evident in Fig. 3. Also, the peak-to-valley ratios in the calculated cross sections in Fig. 2 are reduced and become closer to the experimental data. The spectroscopic factors S_{LJ} obtained by normalizing the calculated curves to the experimental cross sections for three angle pairs are listed in Table I, for the $1p_{3/2}$ and $1p_{1/2}$ states. The values of S_{LJ} obtained by using the GN-2 and GN-3 interactions are also listed in Table I. In addition, the average values $\langle S_{LJ}\rangle$ of the spectroscopic factors are compared with the ones obtained from the (e,e′p) and (d,^{3}He) reactions. Although there are some variations of S_{LJ} with angle pairs, the average spectroscopic factors $\langle S_{LJ}\rangle$ are in rather good agreement with the values extracted from the (e,e′p) reaction.

In Figs. 4, 5, and 6, the calculated results with the LF interaction are compared with the cross section and the analyzing power data[15] at angle pairs ($\theta_a=\theta_b=30°$),

TABLE I. Spectroscopic factors S_{LJ} for angle pairs for the $1p_{1/2}$ and $1p_{3/2}$ states of ^{16}O.

^{16}O	Interaction	30°-30°	40°-40°	30°-65°	$\langle S_{LJ}\rangle$
$1p_{1/2}$	LF	1.35	1.39	1.07	1.27
	GN-2	1.21	1.03	0.82	1.02
	GN-3	1.24	1.05	0.86	1.05
	(e,e′p)[a]				1.18
	(d,^{3}He)[b]				2.34
$1p_{3/2}$	LF	2.78	3.29	2.13	2.73
	GN-2	2.33	2.40	1.61	2.11
	GN-3	2.41	2.46	1.75	2.21
	(e,e′p)[a]				2.28
	(d,^{3}He)[b]				3.68

[a]Reference 34.
[b]Reference 35.

($\theta_a = \theta_b = 47°$), and ($\theta_a = 29°$, $\theta_b = 47°$), respectively, for the $1d_{5/2}$ and $1d_{3/2}$ states for the ^{40}Ca($\vec{p}$,2p) reaction. When compared with the calculations by Antonuk *et al.*,[15] our calculated curves bring about very essential improvements in the agreement with analyzing power data in Figs. 5 and 6. In particular, our calculated curve for the analyzing power for the $1d_{5/2}$ state in Fig. 5 is inverted in comparison with the result of Antonuk *et al.* and has a correct sign and shape. However, the disagreements still remain between the calculated cross sections and the experimental data in Figs. 5 and 6. One possible reason for the disagreements may be due to the asymptotic momentum approximation in Eq. (2.12) for the t-matrix element. The spectroscopic factors S_{LJ} obtained by using the LF, GN-2, and GN-3 interactions are listed in Table II, for the $1d_{5/2}$ and $1d_{3/2}$ states. The average values $\langle S_{LJ} \rangle$ of the spectroscopic factors are also listed in Table II, together with the values extracted from the (e,e′p) and (d,^{3}He) reactions. The average values $\langle S_{LJ} \rangle$ are somewhat lower than the values extracted from the (e,e′p) and (d,^{3}He) reactions.

Then, for the first time, we estimate the contributions from each part of the effective N-N interaction to the cross sections and the analyzing powers for the (p,2p) reactions. In Figs. 7 and 8 the calculated results of individual contributions to the cross section of the central (C), spin-orbit (LS), tensor (T), and total ($C+LS+T$) parts in the LF interaction are compared with the data of the cross section at angle pairs ($\theta_a = 30°$, $\theta_b = 65°$) for the $1p_{3/2}$ state for the ^{16}O($\vec{p}$,2p) reaction and ($\theta_a = \theta_b = 30°$) for the $1d_{5/2}$ state for the ^{40}Ca($\vec{p}$,2p) reaction, respectively. There are substantial contributions from the spin-orbit and tensor parts in the LF interaction to the cross section, but the contribution from the central part is quite weak. Similar results are obtained for the $1p_{1/2}$ state for ^{16}O and for the $1d_{3/2}$ state for ^{40}Ca. In Fig. 8 the calculated analyzing power curve for the central part is not drawn because it is very small.

In order to explain the reason for the small contribution of the central part to the cross section, we show the calculated off-shell p-p differential cross sections in terms of

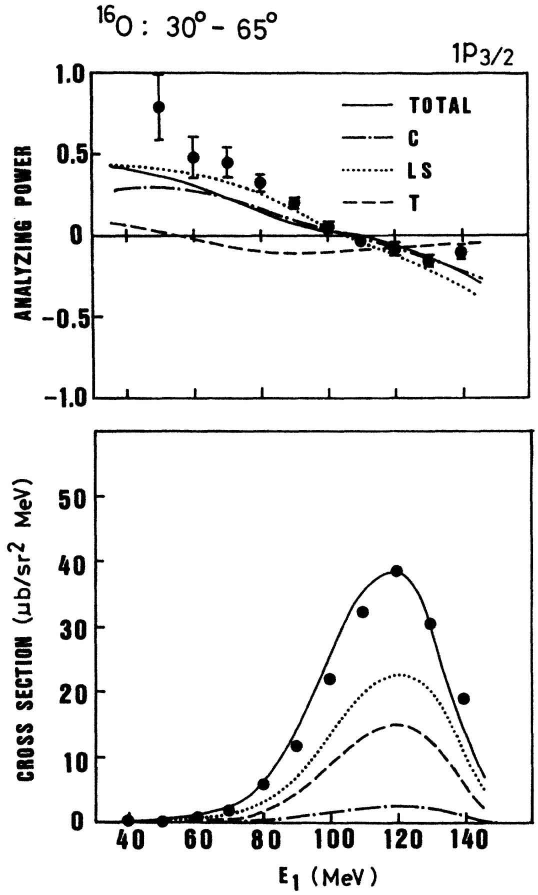

FIG. 7. The calculated results of individual contributions in the LF interaction and the experimental data (Ref. 14) at angle pair ($\theta_a = 30°$, $\theta_b = 65°$) for the $1p_{3/2}$ state for the ^{16}O($\vec{p}$,2p) reaction at $E_p = 200$ MeV. The calculations with central (C), spin-orbit (LS), tensor (T), and total ($C+LS+T$) contributions in the LF interaction are given as dotted-dashed, dotted, dashed, and solid lines, respectively. Also see the caption for Fig. 1. The calculated cross section (total) is normalized to the experimental data.

TABLE II. Spectroscopic factors S_{LJ} for angle pairs for the $1d_{3/2}$ and $1d_{5/2}$ states.

^{40}Ca	Interaction	30°-30°	47°-47°	29°-47°	$\langle S_{LJ} \rangle$
$1d_{3/2}$	LF	3.37	2.00	2.45	2.61
	GN-2	2.91	1.46	1.85	2.07
	GN-3	3.02	1.50	1.94	2.15
	(e,e′p)[a]				3.08
	(d,^{3}He)[b]				3.70
$1d_{5/2}$	LF	4.40	4.21	3.82	4.14
	GN-2	3.71	3.10	2.91	3.24
	GN-3	3.84	3.10	2.97	3.30
	(e,e′p)[a]				4.62
	(d,^{3}He)[b]				4.96

[a]Reference 34.
[b]Reference 36.

the t-matrix element given in the Appendix. We estimate the contributions from each part of the LF interaction to the cross sections. The values of the initial $k_{ab}^{(i)}$ and the final $k_{ab}^{(f)}$ momenta and the momentum transfer $q \equiv q_{ab} = |\mathbf{k}_{ab}^{(f)} - \mathbf{k}_{ab}^{(i)}|$ at the value of $E_1 = 100$ MeV in Fig. 7 for ^{16}O are 1.77, 1.54, and 1.62 fm^{-1}, respectively. Therefore, in Fig. 9 we calculate the off-shell cross sections at the same values of $k_{ab}^{(i)}$ and $k_{ab}^{(f)}$ as a function of q. The point of $q = 1.62$ fm^{-1} is indicated by an arrow on the q axis. As is shown in Fig. 9, the contribution from the central part of the LF interaction to the cross section at $q = 1.62$ fm^{-1} is small and the largest contribution is from the LS part. A similar situation holds for the range of the energy E_1 between 40 and 140 MeV.

Similarly, the values of $k_{ab}^{(i)}$ and $k_{ab}^{(f)}$ and q at the value of $E_1 - E_2 = 15.4$ MeV ($E_1 = 100$ MeV) in Fig. 8 for ^{40}Ca are 1.28, 1.06, and 1.63 fm^{-1}, respectively. Therefore, in Fig. 10 we calculate the off-shell cross sections at the same values of $k_{ab}^{(i)}$ and $k_{ab}^{(f)}$ as a function of q. The point of $q = 1.63$ fm^{-1} is indicated by an arrow on the q axis. As shown in Fig. 10, the contribution from the central part of the LF interaction to the cross section at $q = 1.63$ fm^{-1} is small and the largest contribution is from the tensor part.

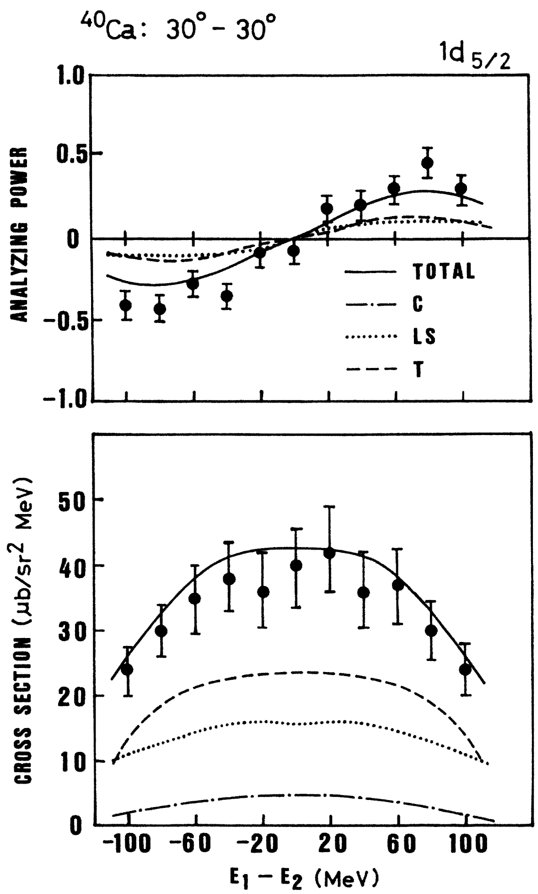

FIG. 8. The calculated results of individual contributions in the LF interaction and the experimental data (Ref. 15) at angle pair ($\theta_a = \theta_b = 30°$) for the $1d_{5/2}$ state for the ^{40}Ca($\vec{p}$,2p) reaction at $E_p = 200$ MeV. Also see the caption for Fig. 7.

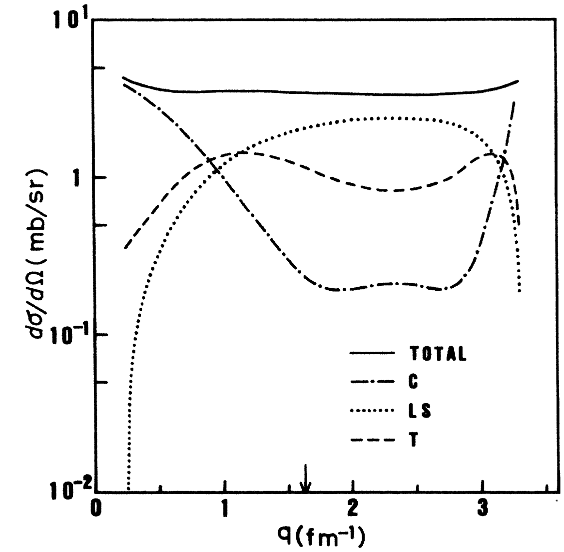

FIG. 9. Calculated off-shell p-p differential cross sections in the c.m. system at the initial $k_{ab}^{(i)} = 1.77$ fm^{-1} and the final $k_{ab}^{(f)} = 1.54$ fm^{-1} momenta. The calculations with central (C), spin-orbit (LS), tensor (T), and total ($C + LS + T$) contributions in the LF interaction are given as dotted-dashed, dotted, dashed and solid lines, respectively. The point of $q = 1.62$ fm^{-1} is indicated by an arrow on the momentum transfer q axis.

In Fig. 11 the calculated results with three types of effective interaction are compared with the data of the cross sections and the analyzing powers at angle pair ($\theta_a = 30°$, $\theta_b = 65°$) for the $1p_{3/2}$ state for the ^{16}O($\vec{p}$,2p) reaction. The calculated curves with the LF interaction and

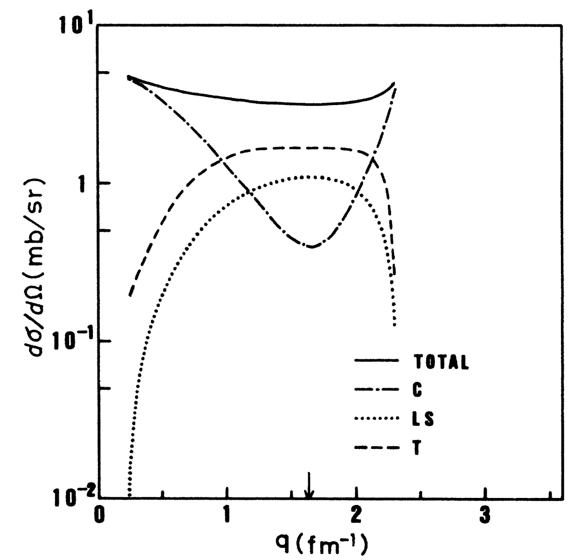

FIG. 10. Calculated off-shell p-p differential cross sections in the c.m. system at the initial $k_{ab}^{(i)} = 1.28$ fm^{-1} and the final $k_{ab}^{(f)} = 1.06$ fm^{-1} momenta. The point of $q = 1.63$ fm^{-1} is indicated by an arrow on the momentum transfer q axis. Also see the caption for Fig. 9.

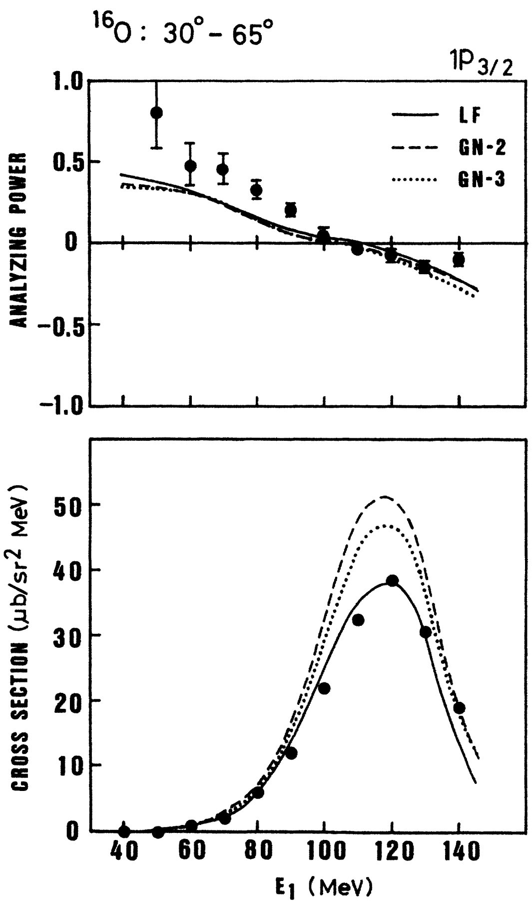

FIG. 11. The calculated results with three types of effective interaction and the experimental data (Ref. 14) of the cross section and the analyzing power at angle pair ($\theta_a=30°$, $\theta_b=65°$) for the $1p_{3/2}$ state for the ^{16}O($\vec{p}$,2p) reaction at $E_p=200$ MeV. The calculated curves with the LF, GN-2, and GN-3 interactions are given as solid, dashed, and dotted lines, respectively.

the GN-2 and GN-3 interactions are given as solid, dashed, and dotted lines, respectively. All curves are calculated with the same spectroscopic factor of 2.13. From the comparison between the cross section with the LF interaction and the one with the GN-2 (GN-3) interaction, it is found that the effect of the Fermi motion (Fermi motion + Pauli blocking) increases the cross section by about 30% (20%), indicating the effects of medium corrections. Then, from the comparision between the curve with the GN-2 interaction and that with the GN-3 interaction, the effect of Pauli blocking decreases the cross section by about 10%, contrary to an increase of less than 10% shown by Miller and Thomas.[11] As shown in Tables I and II, similar results are also obtained for other angle pairs of ^{16}O and for ^{40}Ca, although there are some variations of the extracted spectroscopic factors with angle pairs. Concerning the analyzing powers, it is found that from Fig. 11 the LF, GN-2, and GN-3 interactions provide almost identical results. This result is consistent with that of Miller and Thomas. We obtain similar results for other angle pairs of ^{16}O and for ^{40}Ca.

IV. SUMMARY AND CONCLUSION

Studies of the (p,2p) reaction are entering a new and potentially fruitful period with the beginning of experiments using a polarized beam and with the recent development of effective N-N interactions. We studied analyzing powers and cross sections for the ^{16}O($\vec{p}$,2p) and ^{40}Ca($\vec{p}$,2p) reactions of $E_p=200$ MeV with the effect of the spin-orbit interaction for the distorted waves and with the off-shell effect in proton-proton scattering. The antisymmetrized t-matrix elements are calculated with the effective LF interaction. Our calculations agree well with the experimental data. There are substantial contributions from the spin-orbit and tensor parts in the effective N-N interaction to the cross section, but the contribution from the central part is quite weak. It was found that the density dependent interactions with nuclear medium effects give results almost identical to the LF interaction, except for the magnitude of the cross section.

Our results provide very significant improvements over earlier calculations by the TRIUMF group in which the half-off-shell prescription[8,37] for the p-p scattering matrix element is used. It is shown that the realistic treatment for the calculation of the off-shell t matrix is quite important for the analyzing power. However, still remaining to be studied in more detail is the question of the accuracy of the asymptotic momentum approximation adopted in the present paper. The corrections[38,39] for this approximation may be necessary for us to obtain the precise magnitude and shape of the cross section. The (p,2p) reaction, thereby, can be used in the medium energy region to investigate the structure of a nucleus; in particular, its single-particle properties such as the single particle J value and the spectroscopic factor, and the effective N-N interaction. We hope more experimental data will be available using a polarized proton beam at higher bombarding energies for various target nuclei.

ACKNOWLEDGMENTS

Numerical calculations were carried out at the computer center of the Research Center for Nuclear Physics (RCNP), Osaka University. The authors thank the members of RCNP for granting them use of computer facilities (FACOM M-200) for the present calculations. The authors are very grateful to Professor P. Kitching for comments on the manuscript and to Professor S. Oryu for comments on a half-off-shell prescription based on the Kowalski-Noyes formalism.

APPENDIX

In this appendix we display the antisymmetrized off-shell a-b t-matrix elements in Eq. (2.15), which are given by

$$\langle \mathbf{k}_{ab}^{(f)};\mu_a'\mu_b' \mid \tau_{ab} \mid \mathbf{k}_{ab}^{(i)};\mu_a\mu_b \rangle_a = \sum_{(\gamma_4)} (s_a s_b \mu_a' \mu_b' \mid SM_S')(s_a s_b \mu_a \mu_b \mid SM_S)(t_a t_b \nu_a' \nu_b' \mid TM_T)(t_a t_b \nu_a \nu_b \mid TM_T)\tilde{t}_{k,i}^{S,T} , \quad (A1)$$

where $(\gamma_4)=(k,i,S,T)$, and

$$\tilde{t}_{0,i}^{S,T}=[\widetilde{W}_i^C(q_{ab})+(-1)^{S+T+1}\widetilde{W}_i^C(Q_{ab})]\delta_{M_s,M_{s'}} , \quad (A2)$$

$$\tilde{t}_{1,i}^{S,T}=\sin(\theta)[(i\langle SM_S' \mid S_y \mid SM_S\rangle)/2][Q_{ab}\widetilde{W}_i^{LS}(q_{ab})-(-1)^{S+T+1}q_{ab}\widetilde{W}_i^{LS}(Q_{ab})] , \quad (A3)$$

and

$$\tilde{t}_{2,i}^{S,T}=-4\sqrt{2\pi}\left[\sum_q(-1)^q(S2M_S-q \mid SM_S')\right][\widetilde{W}_i^{TN}(q_{ab})Y_{2q}(\hat{\mathbf{q}}_{ab})+(-1)^{S+T+1}\widetilde{W}_i^{TN}(Q_{ab})Y_{2q}(\hat{\mathbf{Q}}_{ab})] , \quad (A4)$$

with $\mathbf{q}_{ab}=\mathbf{k}_{ab}^{(f)}-\mathbf{k}_{ab}^{(i)}$, $\mathbf{Q}_{ab}=\mathbf{k}_{ab}^{(f)}+\mathbf{k}_{ab}^{(i)}$, and $\cos(\theta)=\hat{\mathbf{q}}_{ab}\cdot\hat{\mathbf{Q}}_{ab}$.

If the radial parts of τ_{ab} are taken to be of Yukawa form,

$$t_{k,i}(r_{ab})=\exp(-x)/x, \quad x=r_{ab}/R_i, \quad k=0,1 \quad (A5)$$

and

$$t_{2,i}(r_{ab})=r_{ab}^2\exp(-x)/x , \quad (A6)$$

then, we obtain

$$\widetilde{W}_i^C(p)=4\pi R_i^3/[1+(pR_i)^2] , \quad (A7)$$

$$\widetilde{W}_i^{LS}(p)=8\pi pR_i^5/[1+(pR_i)^2]^2 , \quad (A8)$$

and

$$\widetilde{W}_i^{TN}(p)=32\pi p^2R_i^7/[1+(pR_i)^2]^3 . \quad (A9)$$

[1]G. Jacob and Th. A. J. Maris, Rev. Mod. Phys. **38**, 121 (1966).
[2]T. Berggren and H. Tyrén, Annu. Rev. Nucl. Sci. **16**, 153 (1966).
[3]D. F. Jackson, in *Advances in Nuclear Physics,* edited by M. Baranger and E. Vogt (Plenum, New York, 1971), Vol. 4, p. 1.
[4]G. Jacob and Th. A. J. Maris, Rev. Mod. Phys. **45**, 6 (1973).
[5]R. Bengtsson, T. Berggren, and Ch. Gustafsson, Phys. Rep. **41**, 191 (1978).
[6]P. Kitching, W. J. McDonald, Th. A. J. Maris, and C. A. Z. Vasconcellos, in *Advances in Nuclear Physics,* edited by J. W. Negele and E. Vogt (Plenum, New York, 1985), Vol. 15, p. 43.
[7]G. Jacob, Th. A. J. Maris, C. Schneider, and M. R. Teodoro, Nucl. Phys. **A257**, 517 (1976).
[8]C. A. Miller, in *Common Problems in Low- and Medium-Energy Nuclear Physics,* edited by B. Castel, B. Goulard, and F. C. Khanna (Plenum, New York, 1979), p. 513.
[9]W. J. McDonald, Nucl. Phys. **A335**, 463 (1980).
[10]P. Kitching, L. Antonuk, C. A. Miller, D. A. Hutcheon, W. J. McDonald, W. C. Olsen, G. C. Neilson, G. M. Stinson, and A. W. Stetz, in *Polarization Phenomena in Nuclear Physics—1980, Part 1,* AIP Conf. Proc. No. 69, edited by G. G. Ohlsen, R. E. Brown, N. Jarmie, W. W. McNaughton, and G. M. Hale (AIP, New York, 1981), p. 568.
[11]C. A. Miller, Nucl. Phys. **A353**, 157c (1981).
[12]N. S. Chant, in *The Interaction Between Medium Energy Nucleons in Nuclei—1982,* AIP Conf. Proc. No. 97, edited by H. O. Heyer (AIP, New York, 1983), p. 205.
[13]N. S. Chant, in *Momentum Wave Functions—1982,* AIP Conf. Proc. No. 86, edited by E. Weigold (AIP, New York, 1982), p. 19.
[14]P. Kitching, C. A. Miller, W. C. Olsen, D. A. Hutcheon, W. J. McDonald, and A. W. Stetz, Nucl. Phys. **A340**, 423 (1980).
[15]L. Antonuk, P. Kitching, C. A. Miller, D. A. Hutcheon, W. J. McDonald, G. C. Neilson, W. C. Olsen, and A. W. Stetz, Nucl. Phys. **A370**, 389 (1981).
[16]W. G. Love and A. Klein, in Proceedings of the Sixth International Symposium on Polarization Phenomena in Nuclear Physics, Osaka, 1985 [J. Phys. Soc. Jpn. Suppl. **55**, 78 (1986)].
[17]W. G. Love and M. A. Franey, Phys. Rev. C **24**, 1073 (1981).
[18]M. A. Franey and W. G. Love, Phys. Rev. C **31**, 488 (1985).
[19]H. V. von Geramb and K. Nakano, in *The Interaction Between Medium Energy Nucleons in Nuclei—1982,* Ref. 12, p. 44.
[20]Y. Kudo and K. Miyazaki, in Proceedings of the Sixth International Symposium on Polarization Phenomena in Nuclear Physics, Osaka, 1985, Ref. 16, p. 620.
[21]D. F. Jackson, Nucl. Phys. **A257**, 221 (1976).
[22]Y. Ikebata and Y. Kudo, in *Proceedings of the 1983 RCNP International Symposium on Light Ion Reaction Mechanism, 1983,* edited by H. Ogata, T. Kammuri, and I. Katayama (RCNP, Osaka University, Ibaraki, Osaka, Japan, 1983), p. 512.
[23]Y. Ikebata and Y. Kudo, Prog. Theor. Phys. **70**, 1457 (1983).
[24]D. F. Jackson and T. Berggren, Nucl. Phys. **62**, 353 (1965).
[25]R. K. Bhowmik, C. C. Chang, J.-P. Didelez, and D. H. Holmgren, Phys. Rev. C **13**, 2105 (1976).
[26]N. S. Chant and P. G. Roos, Phys. Rev. C **27**, 1060 (1983).
[27]L. R. B. Elton and A. Swift, Nucl. Phys. **A94**, 52 (1967).
[28]R. P. Singhal, J. R. Moreira, and H. S. Caplan, Phys. Rev. Lett. **24**, 73 (1970).
[29]J. B. Bellicard, P. Bounin, R. F. Frosch, R. Hofstadter, J. S. McCarthy, F. J. Uhrhane, M. R. Yearian, B. C. Clark, R. Herman, and D. G. Ravenhall, Phys. Rev. Lett. **19**, 527 (1967).
[30]J. R. Comfort and B. C. Karp, Phys. Rev. C **21**, 2162 (1980).
[31]E. Fabrici, S. Micheletti, M. Pignanelli, F. G. Resmini, R. De Leo, G. D'Erasmo, A. Pantaleo, J. L. Escudié, and A. Tarrats, Phys. Rev. C **21**, 830 (1980).
[32]A. Nadasen, P. Schwandt, P. P. Singh, W. W. Jacobs, A. D. Bacher, P. T. Debevec, M. D. Kaitchuck, and J. T. Meek, Phys. Rev. C **23**, 1023 (1981).
[33]H. Sakaguchi, M. Nakamura, K. Hatanaka, A. Goto, T. Noro, F. Ohtani, H. Sakamoto, H. Ogawa, and S. Kobayashi,

Phys. Rev. C **26**, 944 (1982).
[34]S. Frullani and J. Mougey, in *Advances in Nuclear Physics,* edited by J. W. Negele and E. Vogt (Plenum, New York, 1984), Vol. 14, p. 1.
[35]J. D. Cossairt, S. B. Talley, D. P. May, R. E. Tribble, and R. L. Spross, Phys. Rev. C **18**, 23 (1978).
[36]P. Doll, G. J. Wagner, K. T. Knopfle, and G. Mairle, Nucl. Phys. **A263**, 210 (1976).
[37]S. Oryu, Prog. Theor. Phys. **52**, 550 (1974).
[38]N. Austern, Phys. Rev. Lett. **41**, 1696 (1978).
[39]D. F. Jackson, Phys. Scr. **25**, 514 (1982).